JOURNAL OF GEOPHYSICAL RESEARCH, VOL. 101, NO. D23, PAGES 29,395–29,405, DECEMBER 27, 1996

Climatic effect of water vapor release in the upper troposphere

D. Rind, P. Lonergan,[1] and K. Shah[2]

Institute for Space Studies, NASA Goddard Space Flight Center, New York

Abstract. Water vapor is released into the Goddard Institute for Space Studies (GISS) global climate middle atmosphere model at the locations and cruise altitude of subsonic aircraft. A range of water vapor values is used to simulate not only current and 2015 projected emissions but also to provide larger signal-noise ratios. The results show that aircraft water vapor emissions do not significantly affect the model's climate, either at the surface or in situ. With emissions some 15 times higher than the 2015 projection, a small impact is observed, amounting to a few tenths degrees celsius globally and locally, while with emissions 300 times the 2015 values, a global warming of 1°C results. However, with releases this large, only about 5% actually stays in the atmosphere. The larger emissions increase the specific humidity most in the tropical lower troposphere, partly as a result of increased evaporation due to the global warming; at flight altitudes, relative humidity and cloud cover increase at latitudes of emission, and temperature decreases. Surface warming is relatively independent of latitude, and only a slight longitudinal aircraft footprint is found in the warming for the most extreme experiment. Comparison to increased CO_2 experiments of similar magnitude warming shows that the upper tropospheric response is greater in the water vapor release experiments, but the high-latitude surface temperature response is larger with increased CO_2 due to more effective cryospheric feedbacks.

Introduction

Water vapor is among the constituents released by subsonic aircraft in the upper troposphere. Aircraft release 1.25 kg of H_2O for every kilogram of fuel burned [*Lee et al.*, 1994]. In 1990, 1.34×10^{11} kg of fuel were burned [*Wuebbles et al.*, 1993]; hence about 1.67×10^{11} kg of water vapor were released. With expected passenger demand and aircraft increases in mileage, it is estimated 3.8×10^{11} kg of water vapor will be released each year by 2015 [*Baughcum et al.*, 1993].

While aircraft traverse the entire vertical domain of the troposphere, the peak release is expected to occur at the preferred cruising altitude, approximately 10–12 km. This altitude should be relatively unchanged in 2015 for subsonic aircraft [*Baughcum et al.*, 1993] (supersonic aircraft releases maximize around 20 km and may increase in magnitude in the future). The fuel burned in the peak altitude region corresponds to about 60% of the total burned at all altitudes [*Baughcum et al.*, 1993]. The flight paths for subsonic aircraft maximize in the northern hemisphere at 40°–50°N, again a characteristic which will likely remain true through 2015 [*Baughcum et al.*, 1993].

The potential impacts of aircraft water vapor release on climate arise because of the well-known greenhouse capacity of water vapor and because of its ability to form clouds which interact with both shortwave and longwave radiation. The latitude and altitude of this climate forcing is distinctly different from that of most other well-known influences. Increasing concentrations of CO_2, chlorofluorocarbons (CFCs), methane, N_2O, etc. provide a global forcing for their tropospheric lifetimes are sufficiently long to allow for relatively complete tropospheric mixing. Their absorption of longwave radiation provides a significant forcing at all altitudes, especially at the surface where thermal emissions maximize. Stratospheric ozone decreases and volcanic aerosol changes occur at higher altitudes around 20 km. The volcanic eruptions of most importance for climate change produce an eventual global increase in aerosols, while stratospheric ozone changes have so far maximized at high southern latitudes. Tropospheric aerosol changes are of most importance at low altitudes in the northern hemisphere. Possible tropospheric ozone changes are too uncertain to determine their true latitudinal and altitudinal forcing.

Therefore examining the possible influence of aircraft water vapor releases provides the opportunity to study the signature of a relatively unique climate perturbation, one which may be operating today. It will also allow for an estimate of the effects of future increases in subsonic aircraft, a goal of the Subsonic Aircraft Assessment Program (SASS).

There have been several previous studies of the impacts of subsonic water vapor releases. *Schumann* [1993] estimated that subsonic tropospheric emissions of water vapor may well be of the order of 0.02 ppmv over the North Atlantic flight corridor and 0.002 ppmv if mixed uniformly over the troposphere with a lifetime of 9 days. *Shine and Sinha* [1991] estimate that a global increase of 1 ppm for a 50 mbar slab between 400 and 100 mbar would increase surface air temperature by 0.02°C. *Ponater et al.* [1995] investigated the effects of aircraft water vapor releases in simple general circulation model (GCM) experiments. We will compare our results to these studies in the discussion section.

[1]Now at Science Systems and Applications, Inc., New York.

[2]Now at Center for Climate Systems Research, Columbia University, New York.

Paper number 96JD02747.
0148-0227/96/96JD-02747$09.00

Table 1. Water Vapor Release Experiments

Designation	Water Vapor Input, kg/yr	Relation to Aircraft Releases
1	1.17×10^{14}	~700 times "1990"; ~300 times "2015"
2	5.85×10^{12}	~35 times "1990"; ~15 times "2015"
3	5.85×10^{11}	~3.5 times "1990"; ~1.5 times "2015"
4	5.85×10^{10}	~0.35 times "1990"; ~0.15 times "2015"

Note the background water vapor mass in the control run (with no aircraft emissions) is 1.6×10^{16} kg; the background water vapor mass at 12 km is $\sim 1.2 \times 10^{14}$ kg.

Experiments

The study uses the Goddard Institute for Space Studies (GISS) global climate middle atmosphere model (GCMAM) [*Rind et al.*, 1988a, b]. The model extends from the surface to the mesopause, with 23 vertical levels, and 8° × 10° resolution. It has previously been used to investigate the potential climate perturbations due to changes in atmospheric CO_2 [*Rind et al.*, 1990], volcanic aerosols [*Rind et al.*, 1992], UV changes and the quasi-biennial oscillation (QBO) [*Balachandran and Rind*, 1995; *Rind and Balachandran*, 1995], and ozone and water vapor perturbations [*Rind and Lonergan*, 1995]. The last study looked at the possible effect of 2015 supersonic aircraft forcing, but it also included more extreme changes in ozone and water vapor to provide higher signal-to-noise ratios.

Because of uncertainties in the model capabilities for handling tropospheric-stratospheric water vapor exchange, in the following experiments we did not allow the water vapor changes above 100 mb (15–16 km) to influence the climate change results, by keeping values fixed at 3 ppmm. In the most extreme experiment, water vapor above this altitude increased by about 30%. Scaling from the results of *Rind and Lonergan* [1995], in which doubled stratospheric water vapor produced a surface air temperature warming of a few tenths degrees celsius, while a 7% increase produced no consistent response, we estimate that ignoring the additional stratospheric water vapor will underestimate the warming in the most extreme experiment by about 0.1°C (about 10% of the total effect in experiment 1).

We follow the same approach used for the supersonic impacts: we force the model with a range of water vapor releases, encompassing the current and projected aircraft emissions. As water vapor is highly interactive within the troposphere, we must allow for its full capabilities in these experiments. Hence it is released at the primary flight path altitude and location (in both latitude and longitude) and can be advected, rained out, etc. This implies that the ultimate distribution and therefore ultimate climate forcing may have quite a different latitudinal and altitudinal distribution from its input characteristics. Cloud cover changes are also allowed, but effects due to the uncertain aircraft influence on cloud condensation nuclei have not been included. In all experiments, sea surface temperatures are allowed to change so all runs are of 50-year duration to allow for an equilibrium response; water vapor release is constant each year.

Note that this model has a sensitivity of 4°–5°C for doubled atmospheric CO_2 [*Rind et al.*, 1990]. In such experiments, cloud cover acts as a positive feedback, and penetrating convection leads to a large temperature response in the upper troposphere [*Hansen et al.*, 1984]. Models with different sensitivity, cloud cover, and convection schemes may well have results at variance with those shown below, especially if their water vapor and cloud cover feedback is different. Current model sensitivity varies by about a factor of 2 in doubled CO_2 experiments [*International Panel on Climate Control*, 1992]; differences of that degree will not alter the basic conclusions given here.

The experiments are indicated in Table 1. Water vapor was input each hour along the subsonic flight paths. By comparison with the water vapor release values given above, current and 2015 values are between experiments 3 and 4, while experiment 1 is 700 times greater than current releases and 300 times greater than 2015 estimates. The more extreme experiments have greater signal-noise responses, while the smallest release experiments illustrate the noise inherent in model simulations.

Viewed from this perspective, the most extreme experiment added about 1% to the total ambient water vapor in the atmosphere each year. However, the maximum water vapor release occurred at 12 km (approximately 200 mbar) at all latitudes. With the vertical layering used in the GCM, this involved input of water vapor each hour in two model layers, which ranged in zonal mean altitude from 10 to 14 km in the tropics, to 9–13 km at high latitudes. On the global average, the water vapor in these layers is about 1% of the total; hence, experiment 1 was releasing an amount equivalent to the background water vapor at these levels (Table 1). The other experiments are scaled accordingly.

The cumulative latitudinal distribution of the release is shown in Figure 1, compared with current values [*Baughcum et al.*, 1993]. Observations are only from subsonic airliner and cargo aircraft and do not include the releases from military aircraft, which currently account for about 20% of fuel burn [*Wuebbles et al.*, 1993]. Maximum release occurs in northern hemisphere middle latitudes. For the experiments, we use a latitudinal release profile which is an extrapolation of the change from the present to 2015, with 10% greater tropical contribution than in 2015. This is more consistent with the experiments which have a noticeable impact (experiments 1 and 2), whose releases are much larger than that expected to occur in 2015.

The geographical distribution of the release is shown in Figure 2, with the release magnitude indicated by the shading. Maximum releases occur from North America across the

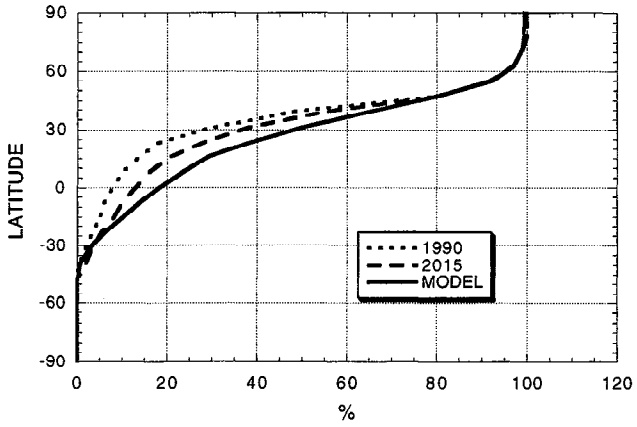

Figure 1. Cumulative latitudinal distribution of fuel burned in observations and projections and water vapor released in the model experiments. Observations and projections are from *Baughcum et al.* [1993].

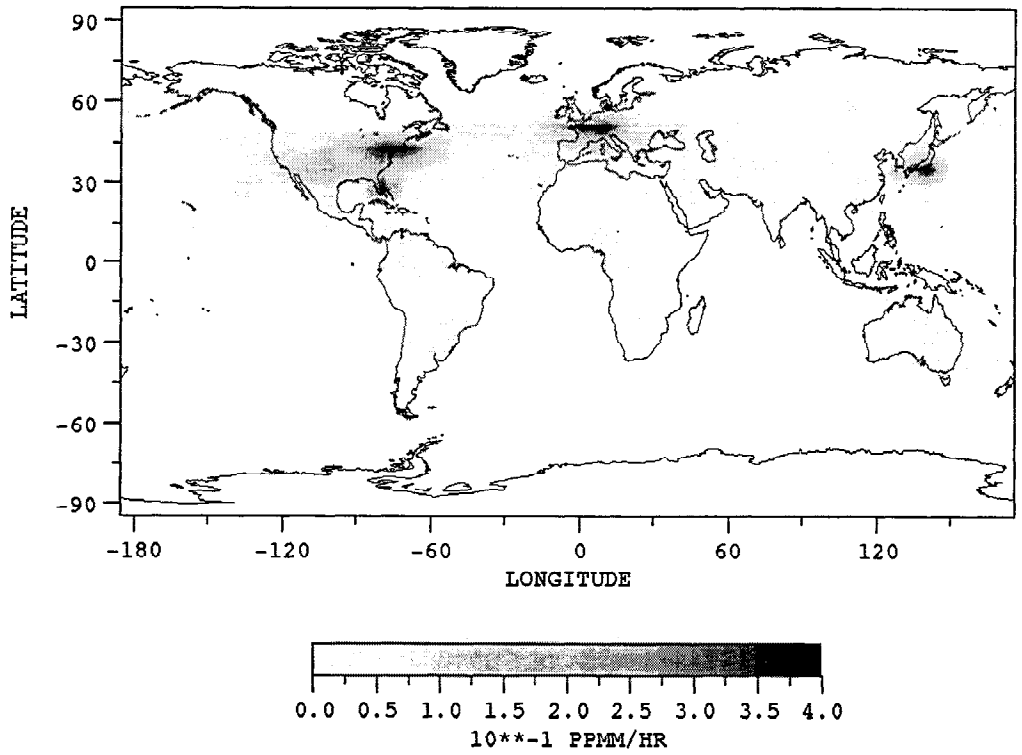

Figure 2. Geographical distribution of water vapor release. Magnitudes are those for experiment 1; the other experiments can be scaled as in Table 1.

North Atlantic to Western Europe, with smaller values across the North Pacific. This scenario is generally applicable for both current and 2015 aircraft flight paths [*Baughcum et al.*, 1993]. The maximum release of 0.4 ppmm/h in experiment 1 can be compared with background values in winter of some 20 ppmm at 12 km. The input therefore does not generally produce immediate saturation and fall out; we estimate below how much actually stays in equilibrium.

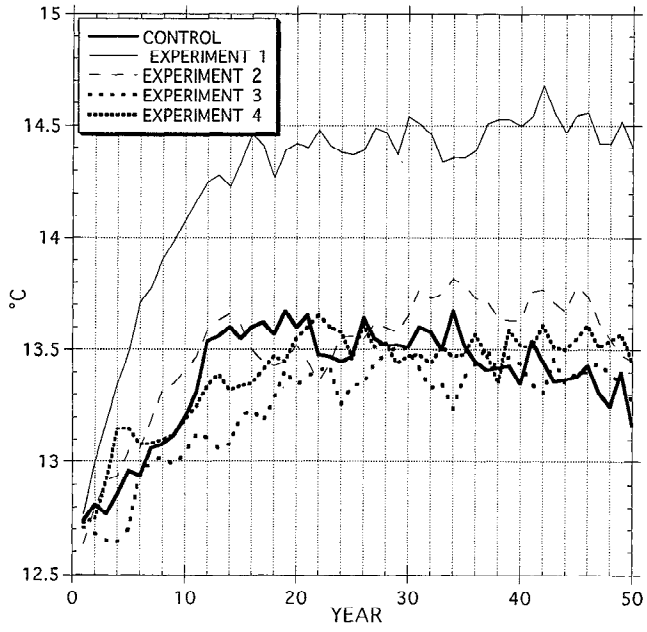

Figure 3. Global annual average surface air temperature as a function of year in the different experiments.

Results

Figure 3 shows the global, annual surface air temperature changes as a function of time for the different experiments and the control. All the runs appear to have stabilized by year 30; unless otherwise indicated, the results shown subsequently will be for years 41–50.

Table 2 gives the changes in relevant climate and radiation variables for the different runs, along with the control run values, averaged for the last 20 years of the experiments. It is evident from Table 2 and Figure 3 that only experiments 1 and 2 have global annual average changes that exceed the noise level (which is indicated by the results from experiments 3 and 4). Experiment 2 is not far above the noise level for some parameters. As discussed by *Rind and Lonergan* [1995], for experiments with small perturbations, changes are often deemed not significant in magnitude relative to the model's interannual standard deviation, even for runs of 50 years, although the sign of the change may be significant in terms of consistency. The warming in both experiments 1 and 2 is larger than the noise level (evident in experiments 3 and 4), and both experiments are consistently warmer than the control for the last 25 years of the simulations (Figure 3). Experiments 3 and 4 show no such consistency. Note that since both current and estimated 2015 aircraft releases fall between experiments 3 and 4, they have no apparent global impact.

Comparing Tables 1 and 2, it appears that in both experiments 1 and 2, the resultant water vapor increase is some 10 times larger than the water vapor being input each year. How

Table 2. Global Annual Changes in the Different Experiments

Parameter	Control	Change in Experiment 1	2	3	4	$\Delta(2 \times CO_2)/4$	Transient
Surface Air Temperature, °C	13.46	1.03	0.24	−0.07	0.07	1.09	1.01
Vertically Integrated Air Temperature, °C	−23.0	1.26	0.29	−0.07	0.08	1.11	0.92
Precipitation, mm/d	3.02	0.086	0.028	−0.01	0.007	0.097	0.07
Evaporation, mm/d	3.00	0.086	0.028	−0.01	0.007	0.097	0.07
Total Cloud Cover, %	46.2	1.14	0.03	0.02	−0.04	−1.7	0.2
Low Cloud Cover, %	35.7	−0.44	−0.17	0.00	−0.07	−0.57	−0.3
High Cloud Cover, %	24.2	1.74	0.12	−0.01	0.00	0.17	0.4
Planetary Albedo, %	31.33	−0.20	−0.09	0.03	−0.04	−0.33	−0.37
Ground Albedo, %	11.39	−0.14	−0.05	0.02	−0.01	−0.27	−0.44
H_2O of Atmosphere, kg	1.6×10^{16}	1.5×10^{15}	3.6×10^{14}	-7.9×10^{13}	1.4×10^{14}	1.2×10^{15}	8.0×10^{14}
Snow Cover, %	10.2	−0.52	−0.11	0.04	−0.02	−0.8	−1.1
Sea Ice, %	3.3	−0.17	−0.07	0.01	−0.02	−0.41	−0.7

Changes are in years.

much of the final change is due to the direct input, and how much due to the evaporation increase which results from the warmer temperatures? We can attempt to estimate the evaporation response to warming by utilizing an experiment in which warming was forced without adding water vapor, such as the doubled CO_2 experiment with the GISS GCM. That simulation produced a 4.2°C warming, approximately 4× that of experiment 1; we therefore normalize the $2 \times CO_2$ results by dividing by a factor of 4 to provide an analog with similar warming magnitude (Table 2). Note that the comparison is somewhat crude; the evaporation response depends upon the latitudinal and altitudinal distribution of the warming, and while the altitudinal distribution is similar, the latitudinal distribution is somewhat different, as will be shown below.

The evaporation response in the doubled CO_2 experiment provided all of the water vapor increase. As shown in Table 2, the (normalized) increase was 1.2×10^{15} kg, or about 80% of the total increase which occurred in experiment 1. This implies that only about 20% (0.3×10^{15} kg) of the increase in experiment 1 was due to the direct water vapor release. Since the total direct water vapor input over the 50 years in this experiment is 5.85×10^{15} kg, only about 5% of this amount apparently stays in the atmosphere. The rest is presumably being removed by precipitation.

In experiment 2, the evaporation increase was about 29% of the normalized $2 \times CO_2$ value, for a water vapor increase of 3.45×10^{14} kg. Hence only about 0.15×10^{14} kg of the total increase (Table 2) was due to the direct input; since the total direct input over the 50 years was 2.92×10^{14} kg, again only about 5% stayed in. The dominance of the (highly nonlinear) warming-induced evaporation effect on atmospheric water vapor over the direct input of water vapor in these experiments helps explains why the model's climate response was not linear: the 20 times larger input in experiment 1 did not produce a similarly larger response in feedbacks or warming compared with experiment 2. A factor of 10 further reduction of water vapor input in experiment 3 was not sufficient to overcome model natural variability, and no warming resulted.

The positive feedbacks evident in experiment 1 and diminishing in experiment 2 are those often noted in the GISS model with warmer climates [*Rind*, 1986]. Low clouds, snow cover, and sea ice decrease, reducing the ground and planetary albedo. Both the water vapor and high cloud cover increases augment the atmospheric greenhouse capacity. By comparison with the one-dimensional analysis in a study by *Hansen et al.* [1984], we estimate that the water vapor change contributes about 0.4°C to the warming in experiment 1, the cloud cover changes about 0.5°C, and the ground albedo change (from snow cover and sea ice decreases) about 0.1°C.

As is evident from Figures 1 and 2, the water vapor release was concentrated at middle latitudes in the northern hemisphere. The resulting specific humidity changes are shown in Figure 4 for experiments 1 and 2. In both experiments, water vapor increases practically everywhere, with a maximum change at low levels in the tropics. The result is influenced by the global warming, initiated by the input water vapor, with increased evaporation adding water vapor where the atmospheric holding capacity is largest. It therefore looks nothing like the water vapor input distribution. The change in equilibrium evaporation, evaporation minus precipitation, and the dynamical moisture convergence as a function of latitude are shown in Figure 5a–5c. The evaporation increase is largest in the tropics. The precipitation minus evaporation change is generally balanced by the change in dynamical moisture convergence, which in equilibrium is adding moisture at high and low latitudes. We return to the dynamical changes responsible for these convergences below.

In both experiments 1 and 2, high latitudes of the northern hemisphere have somewhat larger increases than equivalent latitudes in the southern hemisphere (Figure 4). There is an overall tendency for the patterns of change to be shifted to the north of the equator, rather than being symmetrical about it.

Figure 6 gives the resulting changes in relative humidity. Increases occur in the upper troposphere, maximizing at the latitudes of aircraft water vapor release in contrast to the specific humidity change. Cloud cover changes are given in Figure 7. Maximum increases again occur at the altitude and latitude of water vapor release (although there is substantial tropical response), clearly in experiment 1, and more muted in experiment 2.

The resulting temperature changes are shown in Figure 8. Warming is greatest in the tropical upper troposphere, an indication of the effect of the specific humidity and cloud changes. Cooling occurs in the vicinity of the water vapor release and cloud cover increase, as the clouds radiate more

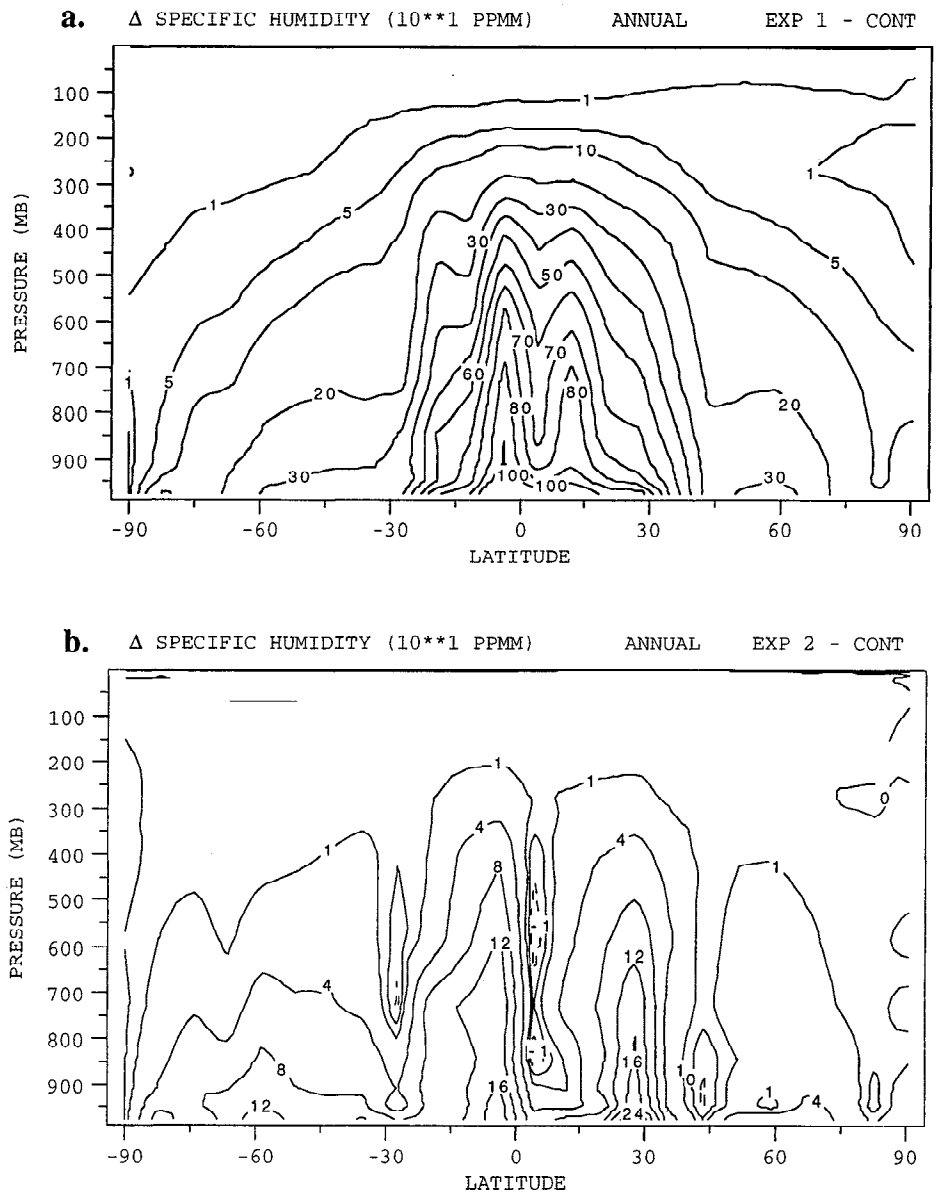

Figure 4. Specific humidity changes in (a) experiment 1 and (b) experiment 2 relative to the control for the last five years of each run.

energy out to space. The resulting small dynamical changes are actually trying to warm this region in response.

The water vapor release had longitudinal as well as latitudinal structure (Figure 2). In experiment 1, there is up to 0.5°C additional warming at longitudes of maximum release. Most other parameters have no zonal structure. The most obvious choice, change in high level cloudiness, has no significant variation between the North Atlantic and North Pacific regions, despite the differences in water vapor release. Zonal advection of water vapor quickly homogenizes the longitudinal distinctions.

In Figure 5d is presented the latitudinal distribution of precipitation change for experiments 1 and 2. Rainfall increases in both the tropics and higher latitudes, in both experiments, with some decrease in the subtropics. Peak changes are of the order of 10% at the respective latitudes. The pattern again is very different from that associated with the direct water vapor release and is the result of the overall evaporation changes and associated dynamical responses. With increased tropical water vapor and precipitation, the annual average tropical circulation cells are intensified. This can be seen in Figure 5e, which shows the vertical velocity changes. Increased upward velocities generally coincide with the precipitation increases, and the subtropical precipitation decreases coincide with increased subsidence. Peak velocity changes are of the order of 20–30%. The mean circulation changes are responsible for the changes in dynamical heat convergence noted earlier (Figure 5c), as the moisture convergences generally coincide with the mass flux convergences that initiate vertical motions.

Comparison With Increased CO_2

It is of interest to compare the climate response to emissions of water vapor in the upper troposphere with the response to increasing CO_2. Both represent potential anthropogenic forcings which should increase with time. A direct comparison of climate response of equal magnitude is not possible, as the

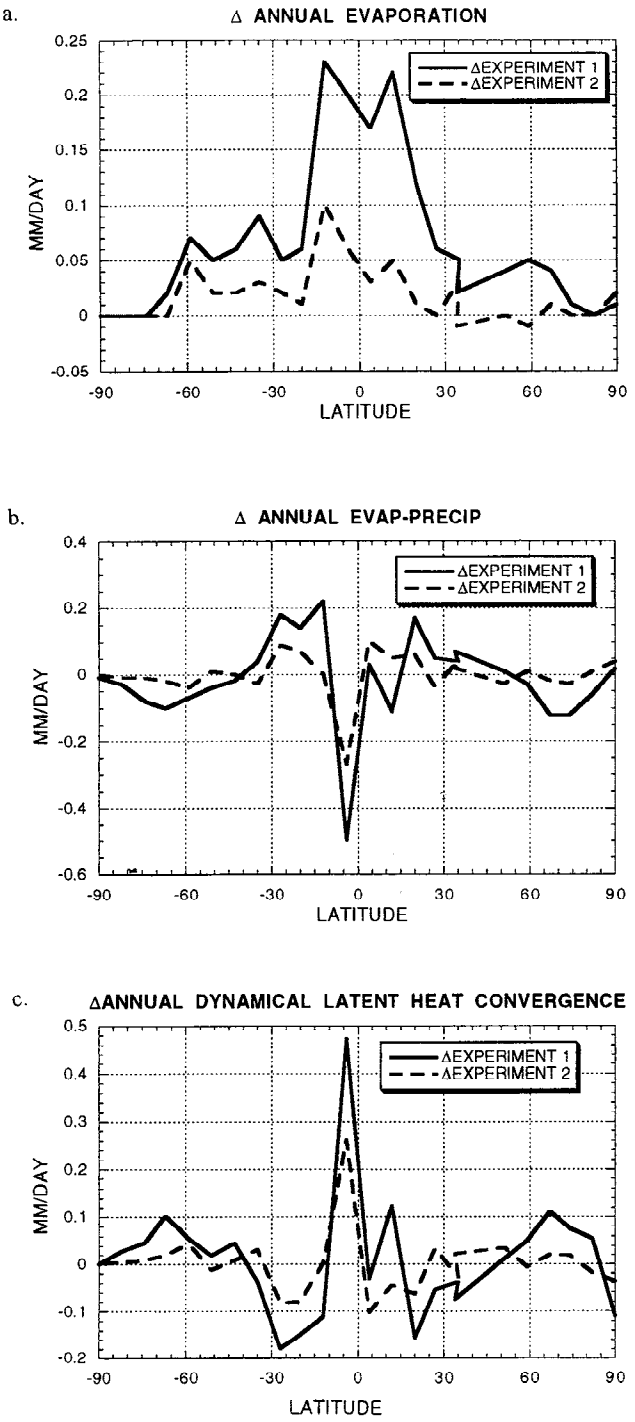

Figure 5. Change in (a) annual average evaporation (b) evaporation minus precipitation, (c) dynamical latent heat convergence, (d) precipitation, and (e) vertical velocity for experiments 1 and 2 during the last 10 years of each run.

equilibrium 2 × CO_2 sensitivity in the GISS model is 4.2°C [*Hansen et al.*, 1984; *Rind*, 1986; *Rind et al.*, 1990], while the most extreme water vapor experiment produced a warming of only 1°C. The transient CO_2 increase experiment [*Hansen et al.*, 1988] passed through a 1°C warming response, but it was not an equilibrium result and was done with a different version of the model (the nine-layer GISS GCM). Comparison of the primary radiative responses in the transient experiment with 1°C warming and 4°C warming suggests that dividing the equilibrium doubled CO_2 4°C warming results by a factor of 4 produces a close enough agreement with the 1°C warming for the comparisons discussed here. Both techniques will be utilized below; it should be recognized that either approach is only approximate.

The relevant global annual changes for the doubled CO_2 experiment, divided by 4, are given in Table 2. For comparison, the changes in the transient experiment passing through a 1°C warming are also shown. With similar surface air temperature changes, most of the other parameters are similar as well, although cloud cover changes are somewhat different.

Comparison of the CO_2 increase experiments with the results from experiment 1 shows that with similar surface air temperature changes, the primary difference is associated with high-level clouds: on a global average, the water vapor release experiment produces a larger increase. In addition, there is a greater change in sea ice and snow cover with increased CO_2.

The surface air temperature change as a function of latitude is shown in Figure 9a. Tropical warming is somewhat higher in the water vapor release experiment, while high-larger warming is greater with increased CO_2. This is somewhat opposite the expected footprint from subsonic aircraft. Also shown is the change in experiment 2; here as well, the response at the latitudes of water vapor release is not amplified.

Changes at 149 mbar in specific humidity (Figure 9b), relative humidity (Figure 9e), and cloud cover (Figure 9c) are also given. The release experiment has much bigger increases, gen-

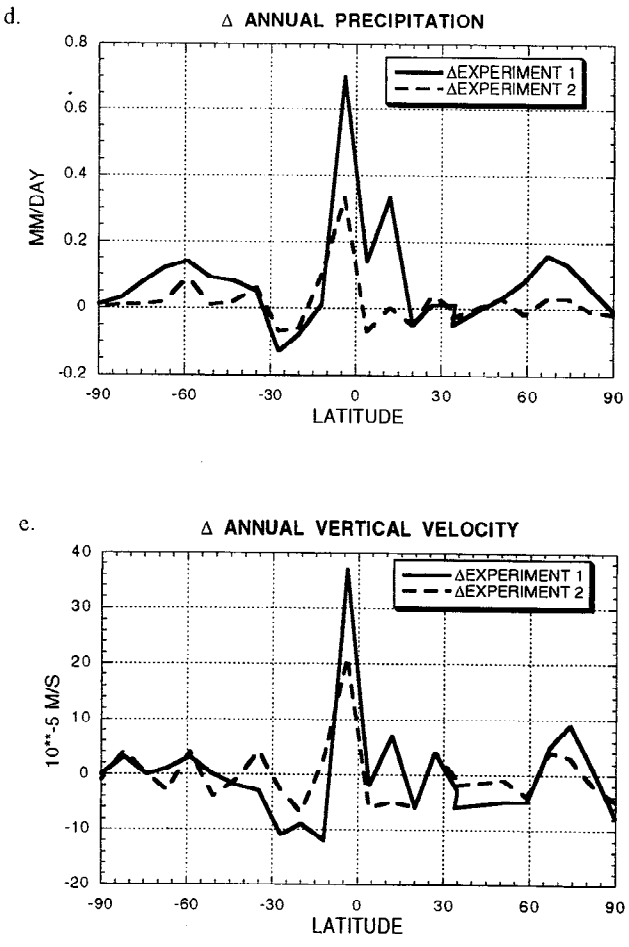

Figure 5. (continued)

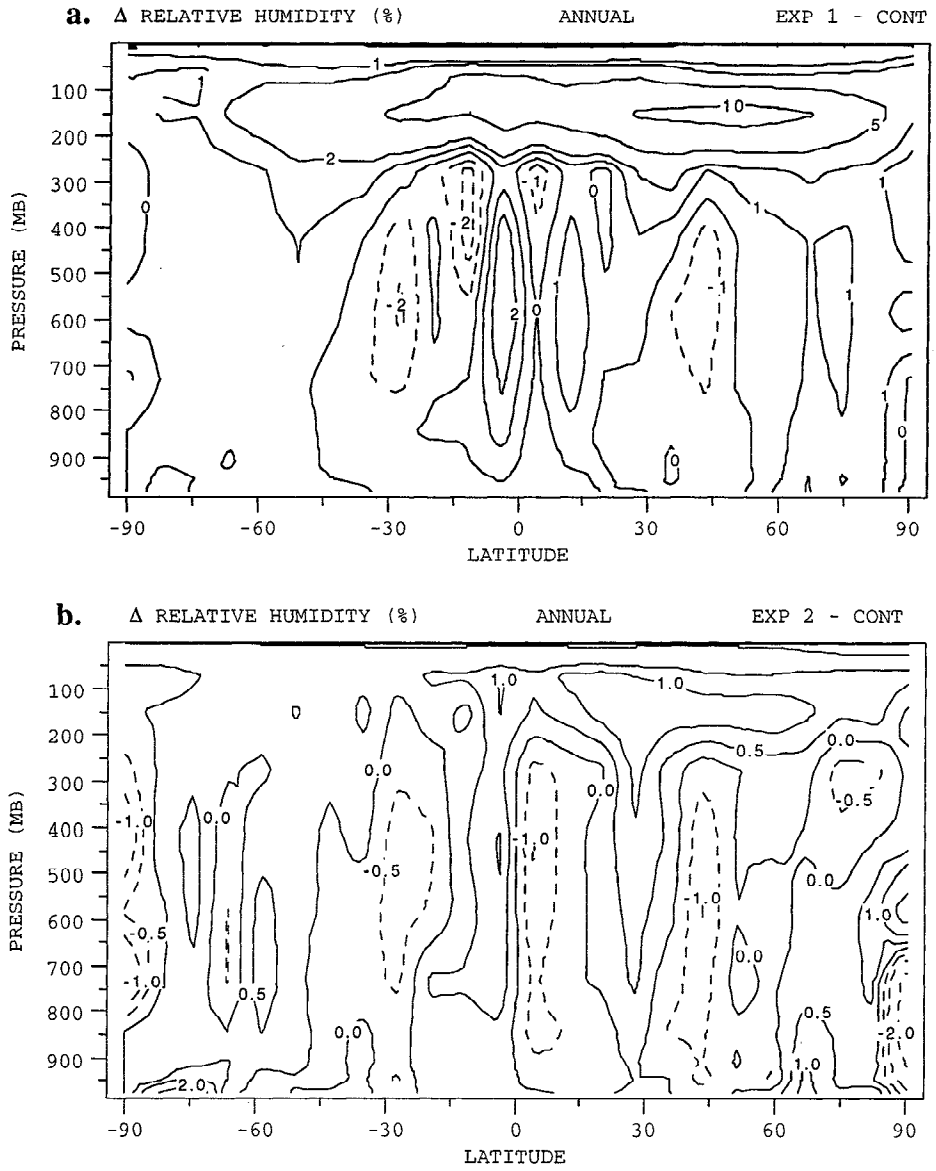

Figure 6. As in Figure 4, except for relative humidity.

erally skewed toward northern hemisphere middle latitudes, while the CO_2 changes are more symmetrical about the equator. (Given the different vertical resolution in the transient CO_2 increase experiment, results are only shown for that run when there are not large gradients across the relevant layers.) Despite such increases, which amplify its high-latitude greenhouse feedback, the water vapor release experiments do not show a greater high-latitude surface air temperature response. The reason is at least partially the result of the sea ice change (Figure 9f), which is greater with increased CO_2; apparently, the direct thermal forcing initiated by the CO_2 results in a larger impact on sea ice. In the doubled CO_2 experiment, the sea ice change was responsible for all of the high-latitude amplification [*Rind et al.*, 1995].

Both the water vapor release and increased CO_2 experiments show decreases in temperature at high latitudes at 149 mbar (Figure 9d). In the aircraft experiment, it is due to the increased radiative loss from the additional high cloud cover. With increased CO_2, it is due more to a decrease in dynamical energy transports, associated with the overall decrease in eddy kinetic energy [*Rind et al.*, 1990], a result which is more prominent in this run since the latitudinal temperature gradient decrease is larger (Figure 9a). Experiment 2 shows the same pattern of response as experiment 1, for the same reason, although the temperature changes are muted.

Discussion and Conclusions

As noted in the Introduction, several previous studies have estimated the impact of subsonic emissions on water vapor and the resulting surface air temperature. *Schumann* [1993] estimated that subsonic tropospheric emissions might increase the tropospheric water vapor content by 2×10^{-3} ppmv. In the control run, the vertically integrated tropospheric water vapor concentration is about 45 ppmv. An increase of 2×10^{-3} ppmv amounts to a change of 0.004%, which is equivalent to 7×10^{11} kg of water vapor. With current releases of 1.67×10^{11} kg/yr, it takes some 6 years to produce the necessary increase if all

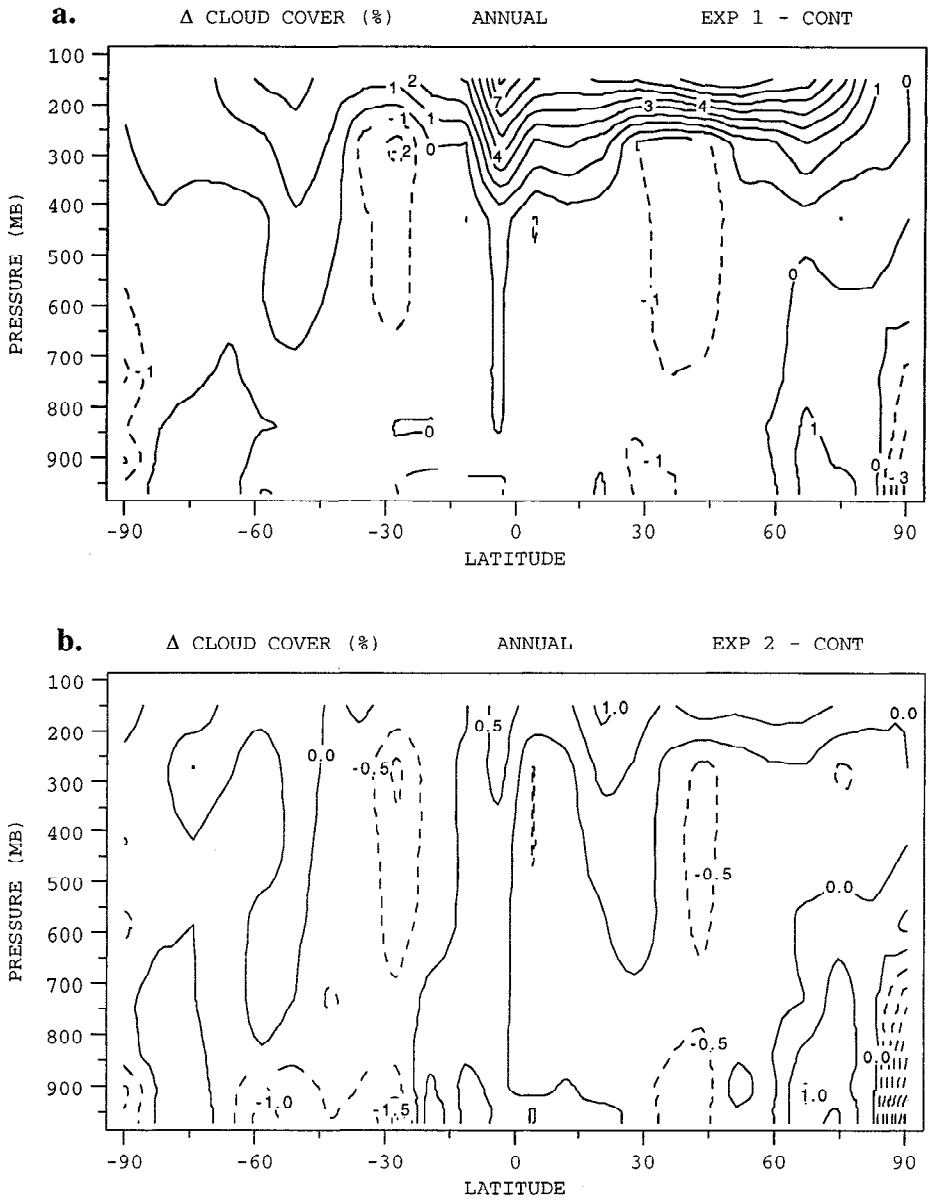

Figure 7. As in Figure 4, except for cloud cover.

were to stay in, a somewhat uncertain response given the model results for experiments 1 and 2. Since the water vapor changes in experiments 3 and 4 were dominated by model variability, we cannot determine how much would stay in. The results from these experiments imply that such an increase would have no noticeable climate effect, as the random fluctuations of temperature and evaporation completely swamp input water vapor values of this magnitude.

Shine and Sinha [1991] estimated that a global increase of 1 ppm for a 50 mbar slab between 400 and 100 mbar would increase surface air temperature by 0.02°C. Such an increase amounts to a water vapor loading of about 2.5×10^{13} kg; this is about 1/10 of the total water vapor change in experiment 2 and produces 1/10 the warming. However, the water vapor change in experiment 2 did not all stay in the upper troposphere, so the proportional response may be somewhat coincidental.

Ponater et al. [1995] used the ECHAM GCM in perpetual January and July mode with specified sea surface temperatures to investigate the effect of aircraft water vapor releases. The fixed sea surface temperatures and the lack of annual cycle limited their ability to investigate the full climate response; nevertheless, their basic conclusion that water vapor releases of some 3 orders of magnitude larger than current aircraft values were necessary to produce a noticeable climate response are roughly comparable to the results here. Since we notice some response with 35 times increase (experiment 2), our model experiments show somewhat greater sensitivity, perhaps due to the sea surface temperature response. In comparison to the latitude/altitude temperature change shown in Figure 8, the most notable difference is that their study found no tropical warming, again perhaps due to the lack of positive water vapor feedback which occurred when the sea surface temperatures warmed. Increased evaporation dominated the atmospheric water vapor gain in both experiments 1 and 2, and the increase was largest in the tropics (Figure 5).

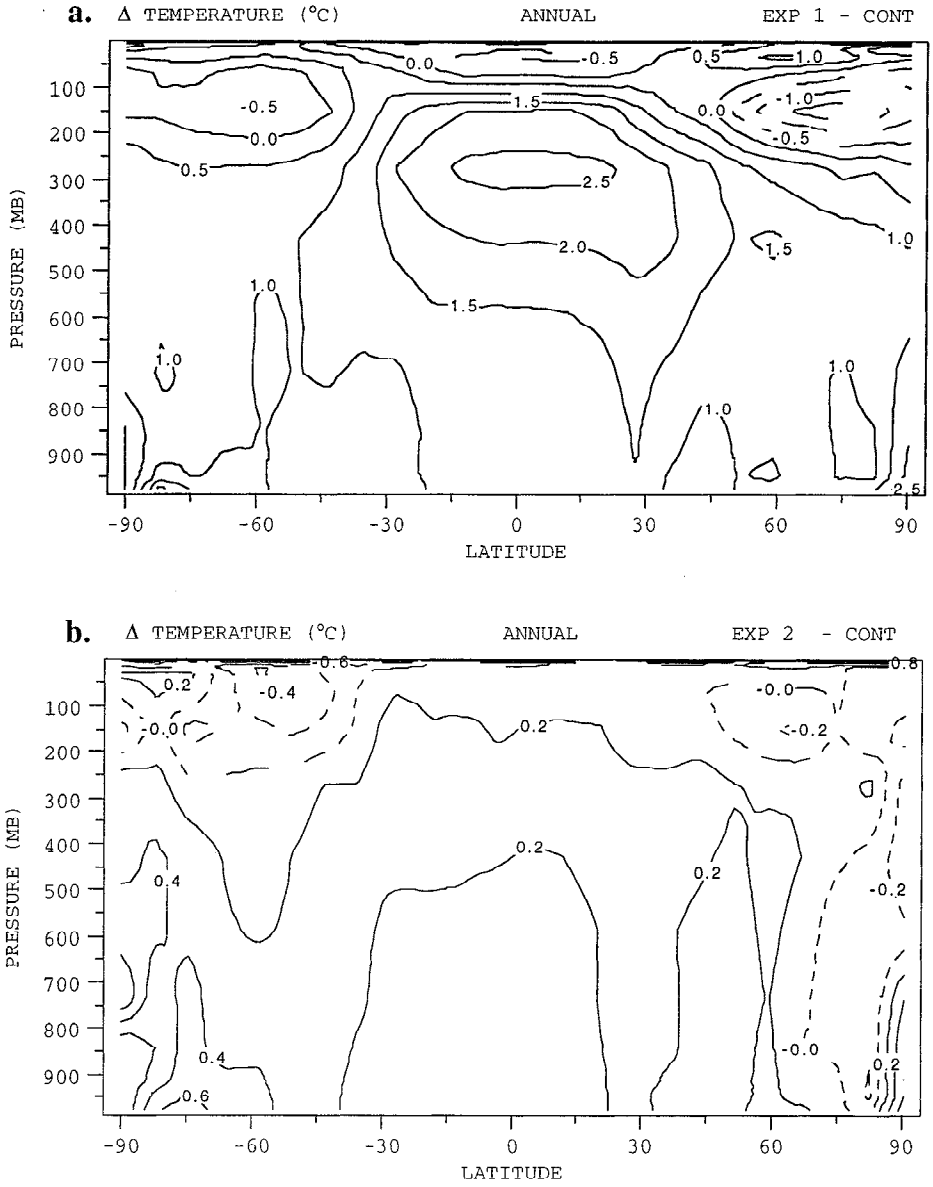

Figure 8. As in Figure 4, except for temperature.

The primary results from these experiments can be summarized in the following manner:

1. Do aircraft water vapor emissions have a noticeable impact on climate?

No, the model experiments indicate that water vapor emissions 35 times greater than current releases, or 15 times greater than those estimated for 2015, are necessary to produce a small equilibrium warming (of about 3 times the model interannual variability). Current estimated-2015 aircraft water vapor releases produce an equilibrium response below the level of model variability.

2. Do large water vapor emissions in the upper troposphere preferentially increase the water vapor along aircraft flight paths?

No, the specific humidity increase is largest in the tropics, where the water holding capacity is greatest. The response is influenced by the system feedbacks, particularly added evaporation in a warming climate.

3. What are the climatic signatures associated with large upper tropospheric water vapor releases along flight paths?

In the latitudinal and altitudinal regions of water vapor release, increases in relative humidity and cloud cover are evident. Associated with the cloud cover increase is a temperature decrease. At the surface, warming is relatively uniform with latitude. There is only a slight longitudinal footprint of small additional warming in regions of maximum flight path release in the most extreme experiment.

4. How does the climatic signature of large upper tropospheric water vapor release compare with that due to increased CO_2?

Given the same global warming, the surface temperature response at the latitudes of maximum release is less than temperature change due to increased CO_2, which is more effective in exciting sea ice and snow cover feedbacks. However, at these same latitudes, increases in upper tropospheric relative humidity and cloud cover are larger in the release experiment.

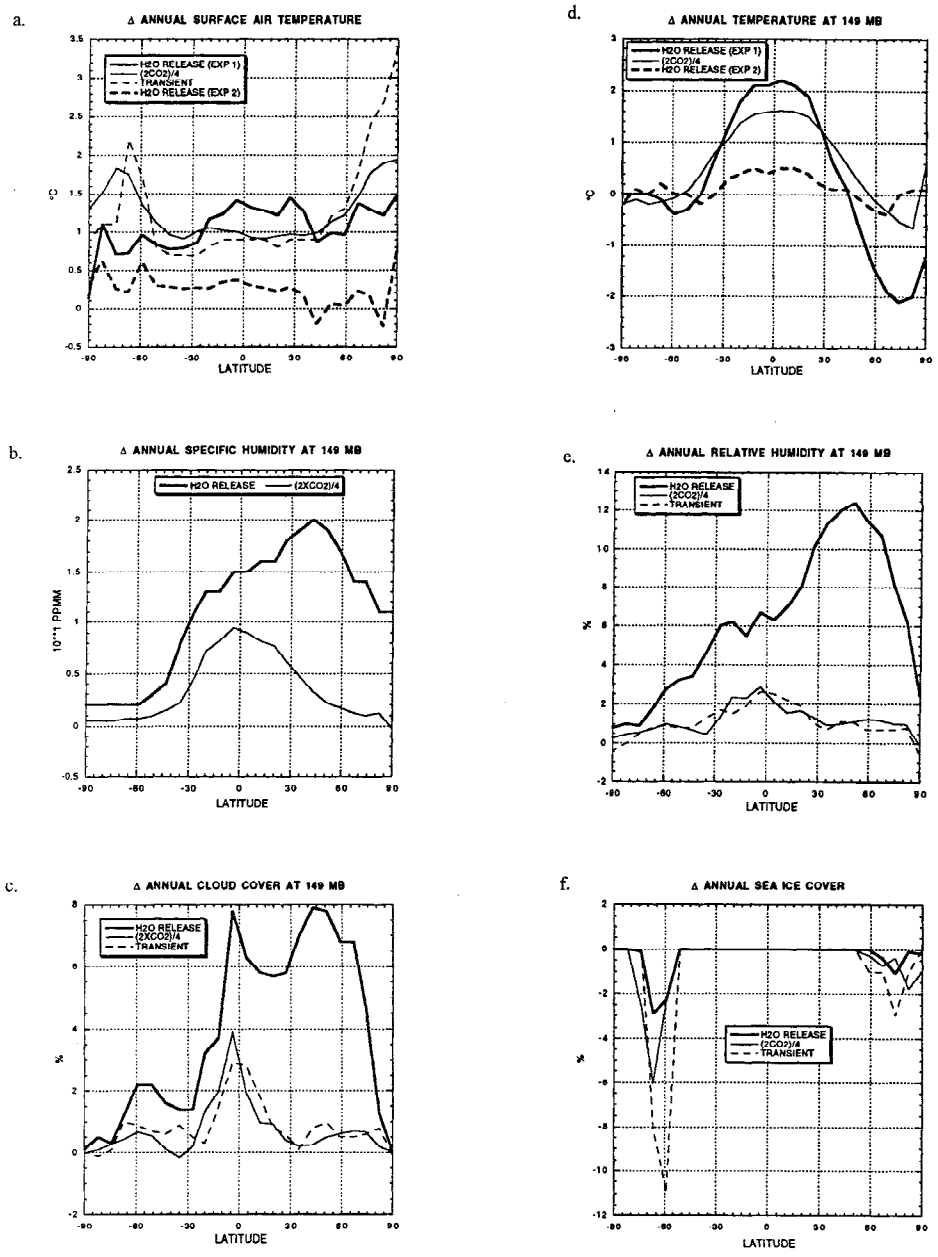

Figure 9. Changes from the control run in annual average values of (a) surface air temperature, (b) specific humidity at 149 mbar, (c) cloud cover at 149 mbar, (d) temperature at 149 mbar, (e) relative humidity at 149 mbar, and (f) sea ice cover in experiments 1 and 2, the doubled CO_2 climate changes divided by 4, and the transient trace gas increase experiment. Results for experiment 2 are shown for temperature to indicate they exhibit the same general pattern as experiment 1, only more muted; results for the transient experiment, with different vertical resolution, are not given when strong gradients occurred across the level of interest.

There are several major caveats associated with this study. Aircraft water vapor releases occur along narrow flight paths. While there is undoubtedly subsequent dispersal, the impact of a concentrated water vapor release over a small area will likely produce more extreme cloud cover changes than the same water vapor release averaged over large grid boxes. It is uncertain, however, whether the time-averaged results would be any different. Only 60% of the subsonic water vapor release occurs in the upper troposphere, with the rest taking place on ascent to or descent from that level, while these experiments put all of it directly into the upper troposphere. However, the model did not keep the water vapor in the upper troposphere anyway, so it is not obvious whether a less concentrated altitudinal release scenario would produce noticeably different effects. An additional uncertainty is the potential impact of other aircraft releases, of particles, for example, which could act as cloud condensation nuclei. Studies to investigate the characteristics and duration of contrails are part of the SASS research program.

Acknowledgments. This work was supported by the NASA Subsonic Aircraft Assessment Program and the NASA Atmospheric Chemistry Modeling and Analysis Program.

References

Balachandran, N. K., and D. Rind, Modeling the effects of UV variability and the QBO on the troposphere-stratosphere system, I, The middle atmosphere, *J. Clim.*, *8*, 2058–2079, 1995.

Baughcum, S. L., D. M. Chan, S. M. Happenny, S. C. Henderson, P. S. Hertel, T. Higman, D. R. Maggiora, and C. A. Oncina, Emissions scenarios development: Scheduled 1990 and projected 2015 subsonic, Mach 2.0 and Mach 2.4 aircraft, in *The Atmospheric Effects of Stratospheric Aircraft: A Third Program Report, NASA Ref. Publ., 1313*, 89–131, Nov. 1993.

Hansen, J. E., A. Lacis, D. Rind, G. Russell, P. Stone, I. Fung, R. Ruedy, and J. Lerner, Climate sensitivity: Analysis of feedback mechanisms, in *Climate Processes and Climate Sensitivity, Geophys. Monogr. Ser.*, vol. 29, edited by J. E. Hanson and T. Takahashi, pp. 130–163, AGU, Washington, D. C., 1984.

Hansen, J., I. Fung, A. Lacis, D. Rind, S. Lebedeff, R. Ruedy, and G. Russell, Global climate changes as forecast by Goddard Institute for Space Studies three-dimensional model, *J. Geophys. Res.*, *93*, 9341–9364, 1988.

International Panel on Climate Control, *Climate Change 1992*, edited by J. T. Houghton, B. A. Callander, and S. K. Varney, 170 pp., Cambridge Univ. Press, New York, 1992.

Lee, S. H., M. Le Dilosquer, H. M. Pasaribu, M. J. Rycroft, and R. Singh, Some consideration of engine emissions from subsonic aircraft at cruise altitudes, in *Impact Emissions From Aircraft and Spacecraft Upon the Atmosphere*, edited by U. Schumann and D. Wurzel, pp. 76–81, Deutsche Forschungsanstalt für Luft-und Raumfahrte.V., Cologne, Germany, 1994.

Ponater, M., S. Brinkop, R. Sausen, and U. Schumann, Simulating the global atmospheric response to aircraft water vapour emissions and contrails—A first approach using a GCM, *Rep. 43*, 40 pp., Inst. fur Phys. der Atmos., Wessing, Germany, 1995.

Rind, D., The dynamics of warm and cold climates, *J. Atmos. Sci.*, *43*, 3–24, 1986.

Rind, D., and N. K. Balachandran, Modeling the effects of UV variability and the QBO on the troposphere-stratosphere system, II, The troposphere, *J. Clim.*, *8*, 2080–2095, 1995.

Rind, D., and P. Lonergan, Modeled impacts of stratospheric O_3 and H_2O perturbations with implications for HSCT aircraft, *J. Geophys. Res.*, *100*, 7381–7396, 1995.

Rind, D., R. Suozzo, N. K. Balachandran, A. Lacis, and G. L. Russell, The GISS global climate/middle atmosphere model, I, Model structure and climatology, *J. Atmos. Sci.*, *45*, 329–370, 1988a.

Rind, D., R. Suozzo, and N. K. Balachandran, The GISS global climate/middle atmosphere model, II, Model variability due to interactions between planetary waves, the mean circulation and gravity wave drag, *J. Atmos. Sci.*, *45*, 371–386, 1988b.

Rind, D., R. Suozzo, N. K. Balachandran, and M. Prather, Climate change and the Middle Atmosphere, I, The doubled CO_2 climate, *J. Atmos. Sci.*, *47*, 475–494, 1990.

Rind, D., N. K. Balachandran, and R. Suozzo, Climate change and the middle atmosphere, II, The impact of volcanic aerosols, *J. Clim.*, *5*, 189–208, 1992.

Rind, D., R. Healy, C. Parkinson, and D. Martinson, The role of sea ice in $2 \times CO_2$ climate model sensitivity, 1, The total influence of sea ice thickness and extent, *J. Clim.*, *8*, 448–463, 1995.

Schumann, U., On the effect of emissions from aircraft engines on the state of the atmosphere, *AGARD Conf. Proc.*, *536*, 1–19, 1993.

Shine, K. P., and A. Sinha, Sensitivity of the Earth's climate to height-dependent changes in the water vapour mixing ratio, *Nature*, *354*, 382–384, 1991.

Wuebbles, D. J., S. L. Baughcum, M. Metwally, and R. K. Seals Jr., Fleet operational scenarios, in *The Atmospheric Effects of Stratospheric Aircraft: Interim Assessment Report of the NASA High-Speed Research Program, NASA Ref. Publ., 1333*, 39–53, June 1993.

P. Lonergan, Science Systems and Applications Inc., 2880 Broadway, New York, NY 10025.

D. Rind, Institute for Space Studies, NASA Goddard Space Flight Center, New York, NY 10025.

K. Shah, Center for Climate Systems Research, Columbia University, 2880 Broadway, New York, NY 10025.

(Received November 15, 1995; revised May 25, 1996; accepted August 14, 1996.)